Functional Association of Arabidopsis CAX1 and CAX3 Is Required for Normal Growth and Ion Homeostasis[1]

Ning-Hui Cheng, Jon K. Pittman[2], Toshiro Shigaki, Jinesh Lachmansingh, Sherry LeClere, Brett Lahner, David E. Salt, and Kendal D. Hirschi*

United States Department of Agriculture/Agricultural Research Service, Children's Nutrition Research Center (N.-H.C., J.K.P., T.S., J.L., S.L., K.D.H.), and Department of Human and Molecular Genetics (K.D.H.), Baylor College of Medicine, Houston, Texas 77030; Department of Horticulture and Landscape Architecture, Purdue University, West Lafayette, Indiana 47907 (B.L., D.E.S.); and Vegetable and Fruit Improvement Center, Texas A&M University, College Station, Texas 77845 (K.D.H.)

Cation levels within the cytosol are coordinated by a network of transporters. Here, we examine the functional roles of calcium exchanger 1 (CAX1), a vacuolar H^+/Ca^{2+} transporter, and the closely related transporter CAX3. We demonstrate that like CAX1, CAX3 is also localized to the tonoplast. We show that *CAX1* is predominately expressed in leaves, while *CAX3* is highly expressed in roots. Previously, using a yeast assay, we demonstrated that an N-terminal truncation of CAX1 functions as an H^+/Ca^{2+} transporter. Here, we use the same yeast assay to show that full-length CAX1 and full-length CAX3 can partially, but not fully, suppress the Ca^{2+} hypersensitive yeast phenotype and coexpression of full-length CAX1 and CAX3 conferred phenotypes not produced when either transporter was expressed individually. In planta, *CAX3* null alleles were modestly sensitive to exogenous Ca^{2+} and also displayed a 22% reduction in vacuolar H^+-ATPase activity. *cax1/cax3* double mutants displayed a severe reduction in growth, including leaf tip and flower necrosis and pronounced sensitivity to exogenous Ca^{2+} and other ions. These growth defects were partially suppressed by addition of exogenous Mg^{2+}. The double mutant displayed a 42% decrease in vacuolar H^+/Ca^{2+} transport, and a 47% decrease in H^+-ATPase activity. While the ionome of *cax1* and *cax3* lines were modestly perturbed, the *cax1/cax3* lines displayed increased PO_4^{3-}, Mn^{2+}, and Zn^{2+} and decreased Ca^{2+} and Mg^{2+} in shoot tissue. These findings suggest synergistic function of CAX1 and CAX3 in plant growth and nutrient acquisition.

Endomembrane Ca^{2+} efflux transporters provide three critical functions in plants (Sanders et al., 2002). First, following Ca^{2+} release, efflux systems reset Ca^{2+} levels to resting levels, thereby terminating the Ca^{2+} signal. Second, they load Ca^{2+} into compartments such as the vacuole to deposit Ca^{2+} for future release. Third, they supply Ca^{2+} to various organelles to support biochemical functions. For many Ca^{2+} transport pathways into endomembrane compartments, the transfer of Ca^{2+} is directly coupled to proton movement (Sze et al., 1999; Gaxiola et al., 2002). While plant scientists have long recognized the importance of H^+ and Ca^{2+} gradients across endomembranes, the array of different types of Ca^{2+} transporters, along with their functional redundancy, has hindered our ability to study the physiological impact of perturbing Ca^{2+} transport function.

At the whole-plant level, it has been well documented that there is a complex interplay among various ions (Marschner, 1995). For example, supplemental Ca^{2+} is known to mitigate the adverse effects of salinity on plant growth (Epstein, 1972). Recently, it has become possible to measure the sum total of the plant's mineral nutrient and trace element composition, termed the ionome (Lahner et al., 2003). The ionome phenotypes now allow investigators to assess how alterations in specific transporters affect these ionic relationships.

Ca^{2+} and other cations can accumulate to millimolar levels in the vacuole, whereas the concentrations of these cations are maintained in the micromolar range in the cytosol (Taiz et al., 1990; Marty, 1999). In the case of Ca^{2+}, this concentration gradient is established in part by high-capacity H^+/Ca^{2+} exchange and via Ca^{2+} pumping directly energized by ATP hydrolysis (Sze et al., 2000). The driving force for cation antiport activity is the pH gradient generated by two electrogenic proton pumps located on the membrane, an ATPase and a pyrophosphatase (PPase; Sze et al., 1999). In principle, the proton pumps and the H^+/cation exchangers can both dramatically alter the cation content of the vacuoles.

Plant H^+/Ca^{2+} exchangers were cloned by the ability of N-terminal truncated versions of the proteins to function in yeast (*Saccharomyces cerevisiae*) mutants

[1] This work was supported by the U.S. Department of Agriculture/Agricultural Research Service (under Cooperative Agreement 58–6250–6001) and by the National Science Foundation (grant nos. 020977 and 0077378–DBI to D.E.S.).

[2] Present address: Faculty of Life Sciences, University of Manchester, 3.614 Stopford Building, Oxford Road, Manchester M13 9PT, UK.

* Corresponding author; e-mail kendalh@bcm.tmc.edu; fax 713–798–7078.

Article, publication date, and citation information can be found at www.plantphysiol.org/cgi/doi/10.1104/pp.105.061218.

defective in vacuolar Ca^{2+} transport (Hirschi et al., 1996; Ueoka-Nakanishi et al., 2000; Pittman and Hirschi, 2001). These genes were originally termed Ca^{2+} exchangers (CAX), and the N-terminal truncated versions called short-CAX (sCAX). Arabidopsis (*Arabidopsis thaliana*) appears to have many putative CAX transporters (Mäser et al., 2001) that may possess different biochemical properties. For example, N-terminal truncated versions of CAX1 and CAX2 can function in yeast as H^+/Ca^{2+} exchangers; CAX1 is a high-capacity Ca^{2+} transporter, whereas CAX2 has a lower capacity for Ca^{2+} and appears to transport other metals (Pittman and Hirschi, 2003). Interestingly, both full-length and N-terminally truncated CAX3, which is the CAX transporter most similar to CAX1 (77% identical at the amino acid level), do not apparently function in yeast as vacuolar Ca^{2+} transporters (Shigaki and Hirschi, 2000). Understanding the localization, expression, and functional properties of these different CAX transporters is an important element in determining how plants regulate ion homeostasis.

Recently, *CAX1* deletion mutants have provided insight into the physiological function of this vacuolar cation/H^+ antiporter (Catala et al., 2003; Cheng et al., 2003). Biochemical analysis of Ca^{2+} transport in *cax1* indicated that under specific growth conditions, 50% of the H^+/Ca^{2+} antiport activity in wild-type Arabidopsis was mediated by CAX1. Interestingly, the *cax1* lines displayed increased vacuolar Ca^{2+}-ATPase activity and increased expression of *CAX3* and *CAX4*. Despite these alterations in vacuolar transport activities, the effects of *CAX1* deletion on plant growth were subtle. However, ectopic expression of the N-terminal truncated CAX1 in tobacco (*Nicotiana tabacum*) caused increased Ca^{2+} accumulation, whereas the expression of the N-terminal truncated CAX2 resulted in increased accumulation of Ca^{2+}, Cd^{2+}, and Mn^{2+} (Hirschi, 1999; Hirschi et al., 2000). The genetic redundancy and functional compensation necessitate the analysis of multiple *CAX* mutants to fully understand the contribution of H^+/Ca^{2+} antiport in physiological processes (Hirschi, 2003).

In this study, we tentatively determine the membrane localization of CAX3 and characterize the tissue expression of *CAX1* and *CAX3*. We further characterize the function of full-length CAX1 and CAX3 by utilizing yeast expression assays and report the isolation of *CAX3* knockout mutants and describe the phenotypes of these plants at the whole-plant, molecular, and biochemical level. We then create *cax1/cax3* double mutants and characterize these mutants in a similar manner. We conclude by assessing the impact of *CAX1*, *CAX3*, and *CAX1/CAX3* disruptions on the plant ionome. Collectively, these findings offer unique insights into the functional plasticity of CAX transport and the association between these transporters and H^+ pumps, plant growth, and ion homeostasis.

RESULTS

Subcellular Localization of CAX3

CAX1 appears to localize and function in both yeast and plant vacuolar membranes (Pittman and Hirschi, 2001; Cheng et al., 2003; Carter et al., 2004). When heterologously expressed in yeast cells, both hemagglutinin (HA)-tagged CAX1 and CAX3 colocalize to the yeast vacuolar membrane (Shigaki et al., 2001). In addition, chimeric CAX3, which harbors the 9-amino acid Ca^{2+} transport determinant domain of CAX1, is able to mediate vacuolar Ca^{2+} antiport activity (Shigaki et al., 2001). To further investigate the subcellular localization of CAX3 in plants, microsomal membranes from transgenic lines harboring the HA-tagged CAX3 fusion protein (HA-CAX3) were fractionated. Centrifugation through a linear Suc gradient was first used to compare the distribution of the epitope-tagged transporter in transgenic tobacco (Fig. 1) to that of markers for the tonoplast, plasma membrane (PM), and endoplasmic reticulum (ER) lumen. As shown in Figure 1A, when membrane fractions were screened for the presence of HA-CAX3 accumulation, proteins of approximately 52 kD peaked in fractions of 28% to 34% Suc. The HA-CAX3 protein accumulated in fractions enriched in tonoplast, as indicated by the sedimentation profiles, which overlap with a resident protein (V-ATPase) from this membrane but did not overlap with marker proteins from the ER (immunoglobulin heavy chain binding protein [BiP]) or the PM (PMA1; Fig. 1A). Furthermore, the membrane profile of the proteins detected by anti-HA and anti-V-ATPase was unchanged in gradients pre-

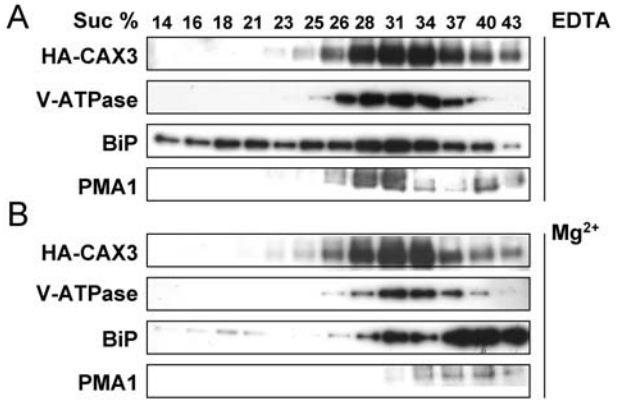

Figure 1. Subcellular localization of CAX3. Immunoblot analysis of CAX3 in transgenic tobacco expressing HA-CAX3. Equal amounts of protein (10 μg) isolated from HA-CAX3-expressing tobacco leaf tissues were separated by SDS-PAGE, blotted, and subjected to western-blot analysis using antibodies against HA (HA-CAX3) and plant membrane markers: the plant ER luminal protein (BiP; StressGen Biotechnologies, Victoria, British Columbia), oat vacuolar ATPase (V-ATPase; Ward et al., 1992), and a PM H^+-ATPase (PMA1; Villalba et al., 1992). HA-CAX3-expressing tobacco leaf tissue membranes were prepared and fractionated in the absence (A) or presence (B) of 1.5 mM $MgCl_2$, as indicated. Numbers above the blots indicate the Suc concentration of each fraction.

pared in the presence of Mg^{2+}, whereas the ER, as detected by anti-BiP, showed a large characteristic Mg^{2+} shift to heavier density fractions (Fig. 1B). This result, together with the localization analysis in yeast, suggests that CAX1 and CAX3 localize to the same endomembrane system, namely, the vacuole.

Expression of *CAX1*::β-Glucuronidase and *CAX3*::β-Glucuronidase in Arabidopsis

RNA-blotting analysis indicated that *CAX3* transcripts were detected in Arabidopsis roots, stems, and flowers, but rarely in leaf tissues (Shigaki and Hirschi, 2000). In comparison, *CAX1* transcripts were highly accumulated in leaf tissues and were also detected in stems and flowers, with low levels of expression in roots (Hirschi, 1999; Cheng and Hirschi, 2003). Given that *CAX3* shows 93% similarity to *CAX1*, cross hybridization might still occur even though gene-specific probes were used in northern-blot analysis (Shigaki and Hirschi, 2000). In order to verify the expression of these two closely related *CAX* members and to gain a more precise profile of the expression pattern of the genes, we constructed *CAX* promoter::β-glucuronidase (GUS) reporters for *CAX1* and *CAX3*. A 2.0-kb genomic DNA sequences upstream of the translation initiation (AUG) codon were amplified by PCR using the promoter-specific primers corresponding to *CAX1* and *CAX3*, respectively. The constructs *CAX3*::GUS and *CAX1*::GUS were transformed into Arabidopsis ecotype Columbia (Col-0). As shown in Figure 2, GUS-staining patterns were comparable to those revealed by RNA-blotting analysis. In *CAX1*::GUS transgenic plants, *CAX1*::GUS expression was predominately detected in leaf tissues (Fig. 2, A and C) and in flowers of the mature plants (Fig. 2, K and L). In cotyledons and young leaves, GUS staining was predominant in the vascular cells (Fig. 2A). Weak GUS staining was seen in roots and stems (Fig. 2, E–G; data not shown), and in the root it was mostly in the vasculature. In comparison with *CAX1*::GUS, strong expression of *CAX3*::GUS was detected in roots, particularly in growing root tips (Fig. 2, H–J). However, GUS signals were rarely detected in leaf tissues and only occasionally detected in stem tissues (Fig. 2, B and D; data not shown). In mature plants, *CAX3*::GUS expression was observed in young flower buds as well as open flowers (Fig. 2M). Both *CAX1*::GUS and *CAX3*::GUS were also expressed in the flowers and siliques (Fig. 2, K–N).

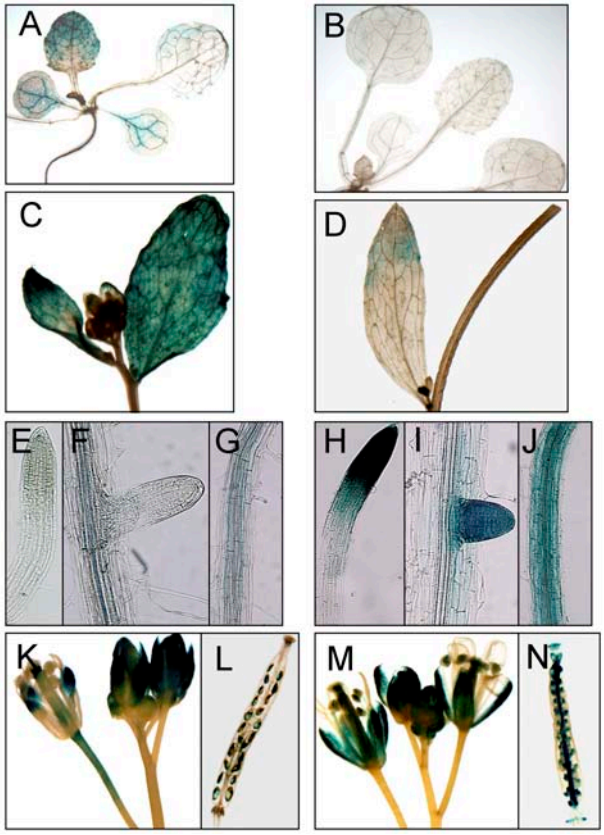

Figure 2. *CAX1* and *CAX3* promoter::GUS expression in transgenic Arabidopsis plants. A, GUS staining in a *CAX1*::*GUS* 10-d-old seedling. Note the preferential GUS expression in the leaf tissues. B, No visible GUS staining in the leaf tissues of the *CAX3*::GUS seedling. C, Strong *CAX1*::GUS expression in young cauline leaves and lateral buds. D, Weak *CAX3*::GUS expression in a cauline leaf and young lateral buds. E to G, No visible GUS staining in primary and lateral roots of *CAX1*::GUS plants. Note the weak signals seen in vascular tissues. H to J, Strong GUS staining in primary and lateral root tips and the root elongation region of *CAX3*::GUS plants. K and L, *CAX1*::GUS expression in flower tissues and young developing embryos. M and N, *CAX3*::GUS expression in flower tissues and young developing embryos.

Expression of CAX1 and CAX3 in Yeast

Previous findings suggest that the N-terminal region of CAX1 acts as an autoinhibitory domain for H^+/Ca^{2+} transport activity when expressed in yeast (Pittman et al., 2002a). To further compare the properties of the CAX transporters with (CAX) and without (sCAX) the putative N-terminal autoinhibitory domain, we cloned these open reading frames into high-copy yeast expression plasmids and expressed them in a yeast strain deficient in vacuolar Ca^{2+} transporters and lacking functional calcineurin (Cunningham and Fink, 1996; Hirschi et al., 1996). This strain (K667) lacks the endogenous vacuolar Ca^{2+}-ATPase PMC1 and vacuolar H^+/Ca^{2+} antiporter VCX1 and thus is defective in vacuolar Ca^{2+} transport, making it unable to grow on high Ca^{2+} media such as 100 mM to 200 mM $CaCl_2$ (Cunningham and Fink, 1996). We examined the growth of yeast cells expressing empty vector control, N-terminally truncated CAX1 and CAX3 (sCAX1 and sCAX3), and full-length CAX1 and CAX3, in media containing 50 mM $CaCl_2$. Under these semipermissive conditions, the vector control-expressing strain grew, albeit poorly; however, both the full-length CAX1 and truncated sCAX1-expressing cells suppressed the Ca^{2+} sensitivity, although the suppression by CAX1 was slightly weaker than sCAX1 (Fig. 3A). Interestingly,

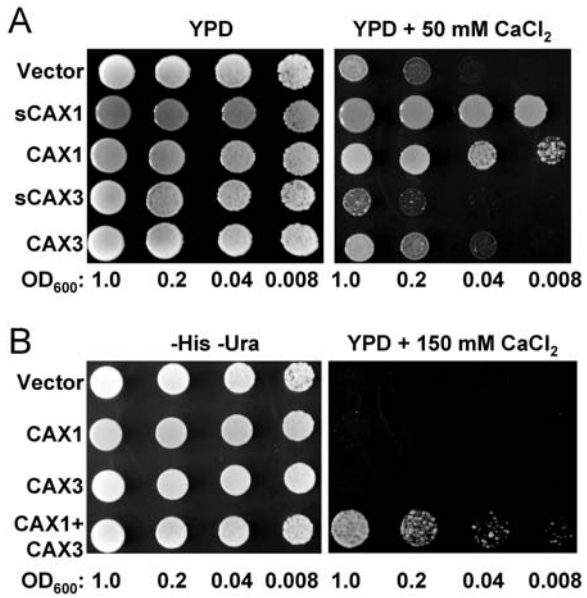

Figure 3. Coexpression of CAX1 with CAX3 in the yeast mutant K667 confers tolerance to high Ca^{2+}. Suppression of Ca^{2+} sensitivity of the *pmc1 cnb vcx1* yeast mutant (K667) by various CAX constructs and their combinations. Saturated liquid cultures of K667 containing various plasmids were diluted to the cell densities, as indicated, and then spotted onto selection medium (−His −Ura) or yeast extract peptone dextrose (YPD) medium and the YPD medium containing 50 mM $CaCl_2$ (A) or 150 mM $CaCl_2$ (B). For the experiment shown in B, CAX1 in a His-selectable plasmid was coexpressed with an empty Ura-selectable plasmid (line 2), CAX3 in a Ura-selectable plasmid was coexpressed with an empty His-selectable plasmid (line 3), and CAX1 and CAX3 were coexpressed in His- and Ura-selectable plasmids, respectively (line 4). For the empty-vector-alone control (line 1), both empty His- and Ura-selectable plasmids were coexpressed.

the CAX3-expressing cells grew weakly under these conditions yet still stronger than vector control, while the sCAX3-expressing cells grew in a manner similar to vector controls (Fig. 3A). In order to determine if there was some association between CAX1 and CAX3, we expressed both transporters simultaneously in this yeast strain, using His- and Ura-selectable yeast expression plasmids, and assayed for phenotypes under conditions that were nonpermissive for growth of each CAX transporter individually. Interestingly, the CAX1+CAX3 coexpression strain was able to grow at 150 mM Ca^{2+}, while yeast expressing the full-length CAX1 or CAX3 individually could not grow (Fig. 3B).

Analysis of *cax3* Null Alleles

Although the structural features of CAX3 are similar to CAX1, the role of CAX3 in Ca^{2+} transport and/or ion homeostasis is still unclear. sCAX1 is able to suppress the Ca^{2+} hypersensitivity of K667 yeast at 50 mM to 200 mM $CaCl_2$, while sCAX3 cannot (Fig. 3A; Shigaki and Hirschi, 2000; Shigaki et al., 2001). In addition, unlike sCAX1-expressing plants (Hirschi, 1999), transgenic tobacco plants expressing sCAX3 did not display altered stress sensitivity (Shigaki et al., 2002; data not shown). To investigate the physiological role of CAX3 in plants, we used PCR screening to identify two T-DNA insertional lines of *CAX3* from two different resources (Sessions et al., 2002; Alonso et al., 2003).

As shown in Figure 4A, we have isolated an Arabidopsis line (*cax3-1*) from the Syngenta Arabidopsis Insertion Library (SAIL) collection (Sessions et al., 2002) in the Col-0 carrying a T-DNA insertion within the *CAX3* open reading frame corresponding to an insertion after the amino acid Arg-193. The T-DNA insertion confers BASTA resistance. A homozygous line was isolated by PCR analysis combined with BASTA selection. We have also isolated another allele, *cax3-2*, from the SALK collection in Col-0 (Alonso et al., 2003). This T-DNA insertion conferred kanamycin (Kan) resistance. Homozygous lines were identified by PCR combined with Kan selection. Sequence analysis of the junction of the T-DNA insert determined that its location was between Phe-115 and Leu-116 (Fig. 4A). These disruptions in *CAX3* did not produce detectable levels of *CAX3* RNA (Fig. 4B), even when high levels (50 mM) of exogenous Ca^{2+} were added, an environmental factor which significantly increases the levels of *CAX3* RNA (Shigaki and Hirschi, 2000). Both the *cax3-1* and the *cax3-2* alleles were backcrossed to the wild type and the F_1 and F_2 progeny were analyzed as previously described (Cheng et al., 2003). The F_2 progeny segregated 3:1 for the antibiotic resistance, indicating both alleles contain a single T-DNA insertion with a functional selection marker (data not shown).

In comparison with wild-type Col-0, Arabidopsis *cax3* null alleles (*cax3-1* and *cax3-2*) do not show any differences in seed germination, plant growth, or flowering time under normal growth conditions (data not shown). However, under Ca^{2+} stress conditions, both *cax3-1* and *cax3-2* had a 25% and 27% reduction in fresh growth weight when compared with wild-type controls and *cax1-1* (Fig. 4C; data not shown).

cax3 Mutants Have Altered H^+-ATPase Activity

We demonstrated previously that deletion of *CAX1* caused an approximately 50% decrease in vacuolar H^+/Ca^{2+} antiport activity compared to wild-type plants (Cheng et al., 2003). This antiport activity was measured following an 18-h pretreatment of the plants with 100 mM $CaCl_2$ prior to harvest and isolation of the vacuolar membrane vesicles. We wished to determine whether deletion of *CAX3* caused a similar alteration in H^+/Ca^{2+} antiport activity. Root tissue was harvested from wild-type, *cax1*, and *cax3* plants pretreated with 100 mM $CaCl_2$, and then H^+/Ca^{2+} antiport activity was measured into vacuolar membrane vesicles by determining the accumulation of 10 μM $CaCl_2$. While antiport activity into vesicles from *cax1* plants was significantly decreased compared to wild type, consistent with our previous results, there was no significant change in activity from *cax3* plants compared to wild type (Fig. 5A).

Another biochemical phenotype of the *cax1* mutant is a reduction in activity of the V-type H^+-ATPase

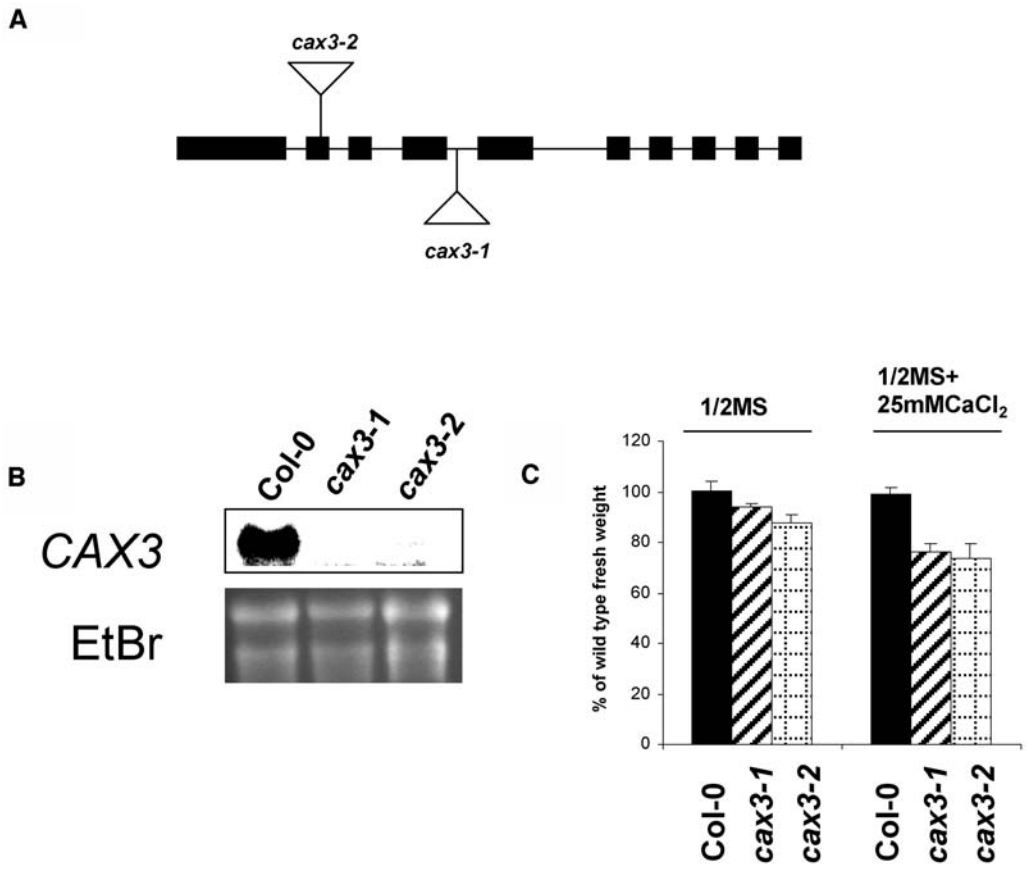

Figure 4. Analysis of *cax3* alleles. A, Diagram of the *CAX3* gene depicting the sites of T-DNA insertions. The approximately 4.0 kb of genomic *CAX3* DNA is represented by nine introns (lines) and 10 exons (boxes). Triangles indicate the sites of the T-DNA locations. The lines harboring these insertions are termed *cax3-1* and *cax3-2*. B, RNA gel-blot analysis of *CAX3* expression in wild-type and *cax3* alleles. Total RNA was extracted from 3-week-old wild-type and *cax3* seedlings pretreated with 50 mM $CaCl_2$ overnight. Ten micrograms of total RNA from each sample was loaded, blotted, and hybridized with a ^{32}P-labeled *cax3*-specific probe. Ethidium bromide (EtBr) staining of the agarose gel is shown as a loading control. C, Reduction of growth mass in *cax3* alleles. Five-day-old seedlings of wild-type (Col-0) and *cax3* alleles were transferred and grown on one-half-strength MS medium in the presence or absence of 25 mM $CaCl_2$ for 10 d. Fresh growth mass of individual seedling for each line was measured. All results are means ± SE ($n \geq 50$). Data are representative of three independent experiments.

(V-ATPase) at the tonoplast (Cheng et al., 2003). We also observed that increased expression of *sCAX1* in the *cax1* plant conferred an increase in V-ATPase activity (Cheng et al., 2003). This phenotype of altered V-ATPase activity was also observed following *CAX3* deletion, when hydrolytic activity of the H^+ pump was measured, although V-ATPase activity was not reduced as greatly in vacuolar membrane vesicles from *cax3* plants (22% reduction in activity) compared to *cax1* plants (38% reduction in activity; Fig. 5B). We found that the *cax1* mutant had no significant alteration in vacuolar H^+-PPase (V-PPase) activity compared to wild type (Cheng et al., 2003). Similarly, the *cax3* mutant had equivalent V-PPase activity to wild-type and *cax1* plants (data not shown).

Impaired Growth and Development in *cax1*/*cax3* Mutant Plants

While *cax1* plants displayed subtle stress tolerances and a late-flowering phenotype, eventually *cax1* plants could grow and produce seeds normally (Cheng et al., 2003). In addition, both *cax1* and *cax3* null alleles were modestly sensitive to exogenous Ca^{2+} (Catala et al., 2003; Fig. 4C). To determine the functional interaction between CAX1 and CAX3, we constructed *cax1/cax3* double-deletion mutants by crossing *cax1* with *cax3* and then selecting for *cax1/cax3* double mutants in the F_2 generation. Homozygous alleles were identified by PCR. We first crossed the *cax1* allele as a maternal with the *cax3* allele as a parental. In the segregation analysis, 16 out of 238 individuals in the F_2 generation were smaller and stunted plants that displayed leaf tip necrosis (Fig. 6; $\chi^2 = 0.09$; $P = 0.79$ for a 1:15 segregation ratio), and all these plants were identified as homozygous for both the *cax1* and *cax3* alleles (see below). Similarly, in the cross between *cax3* (as a maternal) and *cax1* (as a parental), 15 out of 220 individuals in a F_2 population displayed identical phenotypes ($\chi^2 = 0.12$; $P = 0.78$ for a 1:15 segregation ratio). These

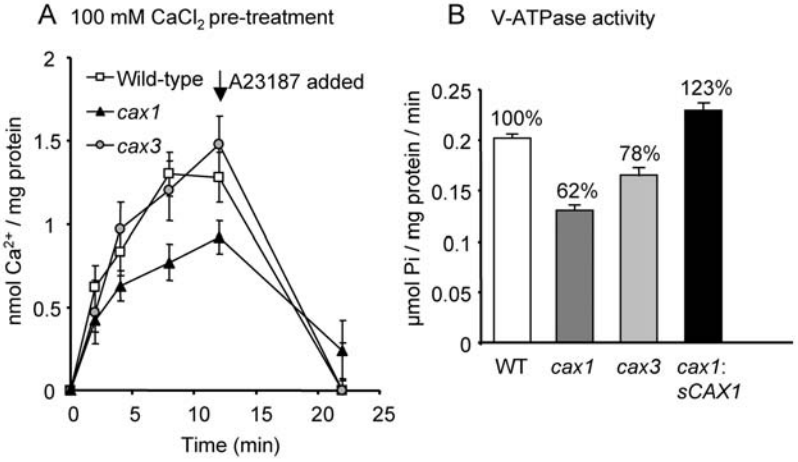

Figure 5. Vacuolar H^+/Ca^{2+} antiport and H^+-ATPase activity in *cax1* and *cax3* mutants. A, Time courses of Mg^{2+}-ATP-energized ΔpH-dependent 10 μM $^{45}Ca^{2+}$ uptake into vacuolar membrane vesicles isolated from wild-type, *cax1*, and *cax3* Arabidopsis plants and determined in the presence of 0.5 mM orthovanadate (a Ca^{2+}-ATPase inhibitor). Eighteen hours prior to harvest and membrane isolation, plants were pretreated with 100 mM $CaCl_2$. H^+/Ca^{2+} antiport activity was determined as the difference between Ca^{2+} uptake in the absence and presence of 5 μM carbonyl cyanide *p*-(trifluoromethoxy) phenylhydrazone (FCCP; protonophore) and net H^+/Ca^{2+} antiport activity is shown after the subtraction of the FCCP background values. The Ca^{2+} ionophore A23187 (5 μM) was added at the 12-min time point and significantly dissipated Ca^{2+} accumulation mediated by H^+/Ca^{2+} antiport when measured at the 22-min time point. B, V-ATPase activity in vacuolar membrane vesicles isolated from wild-type, *cax1*, and *cax3* plants. Activity was determined in the absence or presence of the V-ATPase inhibitor bafilomycin and net activity following subtraction of the bafilomycin background values are shown. Percentages (%) indicate percent of wild-type activity.

analyses indicate that the double-mutant phenotypes result from deletion of both *CAX1* and *CAX3* alleles.

The double deletion of both *CAX1* and *CAX3* had drastic effects on plant growth and development (Fig. 6; data not shown). The *cax1/cax3* plants grew more slowly and were much smaller in comparison with the wild-type and single-mutant plants when grown on soil under continuous light conditions (Fig. 6, A and B), although no difference in germination was observed among the wild type and mutants. In addition, the *cax1/cax3* mutant plants showed necrotic symptoms on the leaf tips and later on the shoot apex (Fig. 6, A, C, and D).

The primary inflorescence stem of *cax1/cax3* plants grew slowly, and eventually necrosis occurred shortly after stem elongation (Fig. 6D). Like the rosette leaves, the cauline leaves also exhibited necrotic lesions at the leaf tips (Fig. 6D). However, the second, third, and fourth shoots continued branching and growing until eventually these floral shoots died. This continued lateral branching and slow growth of the primary stem gave the mutant a bushy appearance (Fig. 6B). Flower set was not significantly altered in the *cax1/cax3* plant compared to wild-type and the single mutants, but silique size and seed numbers were dramatically reduced (Fig. 6, B and E).

cax1/cax3 Double-Null Alleles Are Sensitive to Ion Stresses But Tolerant to Mg^{2+}

Both *cax1* and *cax3* mutant plants have subtle changes in response to ion stresses (Catala et al., 2003; Cheng et al., 2003; Fig. 4C). *cax1* plants are less sensitive to Mg^{2+} in comparison with the wild type (Cheng et al., 2003), while the growth of *cax1* seedlings on high Ca^{2+} media is reduced compared to that of wild-type plants (Catala et al., 2003). The sensitivity of the *cax1/cax3* double mutant to a variety of different ion stresses was tested using conditions as previously described for *cax1* (Cheng et al., 2003). *cax1/cax3* mutant seedlings grew in a manner similar to wild type, and *cax1* and *cax3* single-mutant plants on standard one-half-strength Murashige and Skoog (MS) media (Fig. 6F) and on MS media containing additional Zn^{2+}, Ni^{2+}, Cd^{2+}, and mannitol (data not shown). However, the growth of *cax1/cax3* double-mutant plants was altered in response to a range of excess metal ions, such as Ca^{2+}, Mg^{2+}, and Mn^{2+}. For example, when testing the single mutants and *cax1/cax3* double mutant on media containing 10 mM, 25 mM, and 35 mM $CaCl_2$, *cax1/cax3* mutant plants showed high sensitivity to $CaCl_2$ stress, whereas both *cax1* and *cax3* single-mutant plants were only slightly sensitive to high Ca^{2+} (Figs. 4C and 6G). The *cax1/cax3* lines grew smaller and had darker, curled leaves that displayed leaf tip necrosis when grown on the Ca^{2+}-containing media (Fig. 6, C and G). This phenotype was similar to the plants grown on soil under continuous light (Fig. 6A). Most interestingly, the *cax1/cax3* plants displayed robust growth on medium containing 15 mM $MgCl_2$, which caused growth defects in the control and *cax3* lines (Fig. 6H) and the growth defects of the *cax1/cax3* lines were suppressed by addition of $MgCl_2$ (data not shown). In addition, seed yield was significantly increased by growing

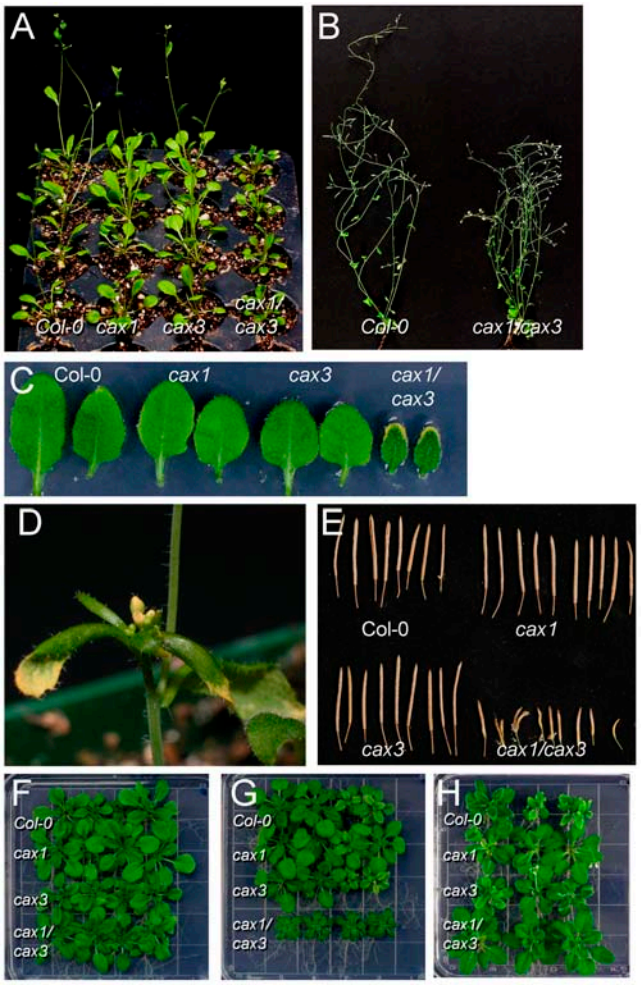

Figure 6. Morphological phenotypes and ion sensitivity of the *cax1/cax3* double-mutant lines. A, Four-week-old wild type (Col-0), *cax1*, *cax3*, and *cax1/cax3* plants were grown on soil under continuous light. The *cax1/cax3* plants grew smaller and showed leaf tip necrosis. B, The mature *cax1/cax3* plants have more branches and appear bushy in comparison with wild-type plants. The *cax1/cax3* double-mutant lines rarely produce normal siliques and seeds. C, The *cax1/cax3* plants have curly dark green leaves showing tip necrosis. D, The *cax/cax3* plant displayed shoot apex necrosis. E, The *cax1/cax3* mature plants have smaller siliques with few seeds. F to H, Five-day-old seedlings of wild type (Col-0), *cax1*, *cax3*, and *cax1/cax3* grown on one-half-strength MS medium were transferred onto one-half-strength MS medium (F), one-half-strength MS medium supplemented with 25 mM $CaCl_2$ (G), and one-half-strength MS medium supplemented with 15 mM $MgCl_2$ and grown for an additional 10 d (H).

plants in nutrient media or by the exogenous application of $MgCl_2$ to the soil (data not shown).

Decreased H^+/Ca^{2+} Antiport and H^+-ATPase Activity in the *cax1/cax3* Mutant

To determine whether H^+/Ca^{2+} antiport activity was further perturbed by deletion of both *CAX1* and *CAX3*, 10 μM $^{45}Ca^{2+}$ antiport activity was compared between wild-type, *cax1*, and *cax3* single mutants, and the *cax1/cax3* double mutant following exogenous $CaCl_2$ pretreatment. Antiport activity into membrane vesicles from *cax1* plants was greatly reduced compared to activity into vesicles from wild-type and *cax3* plants as previously shown (50% reduction; Cheng et al., 2003), while activity from *cax1/cax3* plants was also reduced compared to wild type and *cax3*, but still equivalent to the *cax1* single-knockout plant (Fig. 7A). The *cax1/cax3* double mutant showed a 47% reduction in V-ATPase activity over wild-type activity as compared to the 38% and 22% reductions measured in the *cax1* or *cax3* single mutants, respectively (Figs. 5B and 7B). The *cax1/cax3* mutation had no significant effect on V-PPase activity compared to wild-type plants (data not shown).

Ion Profiling of *cax1*, *cax3*, and *cax1/cax3*

The mutant Arabidopsis lines *cax1*, *cax3*, and *cax1/cax3* were grown in standard potting conditions with 8 h light, alongside wild-type controls. Growth of the double mutant was clearly not as robust as wild-type controls (Fig. 6; data not shown). During the vegetative growth phase shoot tissue was harvested and analyzed for Li^+, B^+, Na^+, Mg^{2+}, PO_4^{3-}, K^+, Ca^{2+}, Mn^{2+}, Fe^{3+}, Co^{2+}, Ni^{2+}, Cu^{2+}, Zn^{2+}, As^{2+}, Se^{2+}, Mo^{2+}, Cd^{2+}, and Pb^{2+} using inductively coupled plasma-mass spectrometry (ICP-MS). Comparison of the ion profiles of each mutant against its respective wild-type controls grown in the same tray revealed several significant changes in the ionomes of both *cax1* and *cax1/cax3*; however, no significant changes were observed in *cax3*. The concentrations of both Mn^{2+} and Zn^{2+} were reduced by 16% and 9% ($P = 0.03$; $n = 13$), respectively, in *cax1*. Furthermore, combination of the *cax1* and *cax3* mutations produced significant changes in PO_4^{3-}, Ca^{2+}, Mn^{2+}, and Zn^{2+} in *cax1/cax3*, with increases in PO_4^{3-}, Mn^{2+}, and Zn^{2+} of 66%, 50%, and 38% ($P = 0.04$; $n = 18$), respectively, and a decrease in Ca^{2+} and Mg^{2+} of 17% and 16% ($P = 0.01$; $n = 18$; Fig. 8). The large increase observed in PO_4^{3-}, Mn^{2+}, and Zn^{2+} levels do not appear to be a cause of the *cax1/cax3* morphological phenotype as this stunted-growth phenotype is not seen in wild-type plants treated with excess concentrations of PO_4^{3-}, Mn^{2+}, and Zn^{2+} (data not shown).

To specifically assay the ionome of *cax1/cax3* in roots, we grew the seedlings on half-strength MS medium plates and harvested shoots and roots after 17-d growth under 10-h-light conditions. As with the soil-grown plants, low Ca^{2+} levels were also observed in shoot tissue of the double mutant grown on plates; however, we saw no pronounced changes in the Ca^{2+} concentrations in roots compared to wild type (data not shown). No alterations were observed for any elements in the *cax1/cax3* roots, although there were also no changes in the shoot of any of the other elements as observed before with the soil-grown plants. This may not be too surprising for PO_4^{3-} and Zn^{2+}, since PO_4^{3-} is dramatically affected by Suc, and Zn^{2+} is affected by PO_4^{3-} (Marschner, 1995).

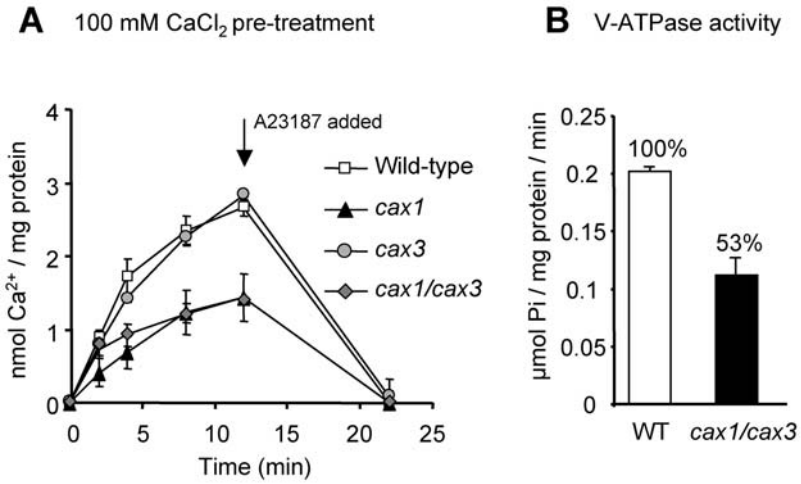

Figure 7. Vacuolar H^+/Ca^{2+} antiport and H^+-ATPase activity in *cax1/cax3* mutants. A, Time courses of Mg^{2+}-ATP-energized ΔpH-dependent 10 μM $^{45}Ca^{2+}$ uptake into vacuolar membrane vesicles isolated from wild-type and *cax1/cax3* Arabidopsis plants pretreated with 100 mM $CaCl_2$. H^+/Ca^{2+} antiport activity was determined as described in the legend to Figure 5. B, V-ATPase activity in vacuolar membrane vesicles isolated from wild-type, *cax1*, *cax3*, and *cax1/cax3* plants. Values for *cax1* and *cax3* activity are from the same experiment as shown in Figure 5B. Activity was determined in the absence or presence of the V-ATPase inhibitor bafilomycin, and net activity following subtraction of the bafilomycin background values is shown.

DISCUSSION

Previously, we and others have shown that the loss of *CAX1*, a putative vacuolar H^+/Ca^{2+} transporter, causes subtle morphological phenotypes (Catala et al., 2003; Cheng et al., 2003). However, *CAX1* is a member of a large multigene family (Mäser et al., 2001). Herein we further analyzed CAX function by heterologous expression in yeast, we continued the characterization of *cax1* and initiated studies to characterize the effects of the loss of *CAX3*, and, furthermore, we described the severe alterations in plant growth and the ionome caused by the *cax1/cax3* double mutation. This work thus illustrated the potential synergy of CAX1 and CAX3 functions and the association between these transporters and plant growth, development, and ion homeostasis.

CAX3 Localization

An HA-tagged version of CAX3 appears to localize to the tonoplast of transgenic Arabidopsis and tobacco (Fig. 1). The Mg^{2+} shift experiment suggests that CAX3 does not localize to the ER (Fig. 1B); furthermore, chlorophyll levels (a chloroplast marker) peaked in 41% to 43% Suc fractions in the presence or absence of Mg^{2+} (data not shown), indicating that CAX3 is not found at this organelle. A previous study revealed that mung bean (*Vigna radiate*) VCAX1-green fluorescent protein is localized to the tonoplast as well as having possible Golgi localization (Ueoka-Nakanishi et al., 2000). In this study, we cannot exclude the possibility from these fractionation experiments that CAX3 may localize to another membrane fraction, such as the Golgi, that also does not shift in the presence of Mg^{2+}. However, localization of HA-CAX3 to the tonoplast when heterologously expressed in yeast (Shigaki et al., 2001) and suppression of the yeast vacuolar Ca^{2+} transport defect mutant phenotype by expression of HA-CAX3 (Cheng et al., 2002), support our conclusion of vacuolar localization. Future CAX-green fluorescent protein fusion studies will be able to confirm the subcellular localization of CAX1 and CAX3 and will also be able to determine whether they are present on identical or different vacuolar subtypes.

Tissue Expression of *CAX1* and *CAX3*

We demonstrate from the expression study that both *CAX1*::GUS and *CAX3*::GUS accumulate in the reproductive organs, such as floral tissues, but differentially accumulate in the vegetative organs (Fig. 2). The most pronounced differences in the expression patterns of *CAX1* and *CAX3* can be seen in the leaf tissue. *CAX3* is expressed at high levels in the roots but at low levels in leaves. In contrast, *CAX1* is expressed at high levels in leaves and low levels in the root vascular cells. However, a notable area of expression overlap has recently been reported in guard cell microarray experiments where *CAX3* expression is enhanced more than 4-fold in the leaf guard cells in response to ab-

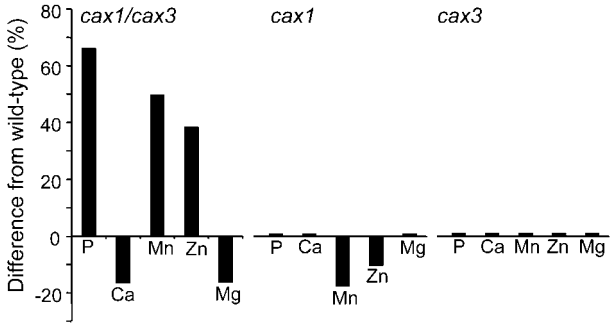

Figure 8. Alterations in the ionome in *cax1/cax3*, *cax1*, and *cax3* mutants. Shoot samples from *cax1/cax3*, *cax1*, *cax3*, and wild-type plants were analyzed for Li^+, B^+, Na^+, Mg^{2+}, PO_4^{3-}, K^+, Ca^{2+}, Mn^{2+}, Fe^{3+}, Co^{2+}, Ni^{2+}, Cu^{2+}, Zn^{2+}, As^{2+}, Se^{2+}, Mo^{2+}, Cd^{2+}, and Pb^{2+} using ICP-MS. Ion profile data of mutants and wild type grown under the same condition were compared, and elements showing a significant difference ($P \geq 0.05$; $n = 13–18$) are shown as black bars as percentage change from the wild type.

scisic acid treatment (Leonhardt et al., 2004; http://www.cbs.umn.edu/arabidopsis). Other microarray data suggest that *CAX3* expression in the aerial portions of the plants during osmotic stress and wounding can reach levels higher than *CAX3* root expression. Thus, our reporter fusions suggest minimal overlap during normal growth in leaf tissue, but emerging data suggest particular stimuli can cause an overlap in *CAX1* and *CAX3* expression. It will be particularly interesting to analyze the overlap in *CAX1* and *CAX3* expression when Ca^{2+} levels are altered. Previous northern-blot analysis has shown that *CAX1* and *CAX3* are up-regulated by exogenous Ca^{2+} (Hirschi, 1999; Shigaki and Hirschi, 2000); however our preliminary experiments show no significant Ca^{2+} induction of the *CAX1*::GUS and *CAX3*::GUS reporters (data not shown). We have tested a variety of different transcriptional fusions of CAX1::GUS and have been unable to see any alterations in GUS activity upon Ca^{2+} exposure (T. Shigaki and K.D. Hirschi, unpublished data). This suggests that the regulatory elements in both the 2 kb of genomic sequences of *CAX1* and *CAX3* are insufficient to alter the reporter during Ca^{2+} treatments. Future experiments will be directed at dissecting the regulatory elements required for Ca^{2+} induction. Despite these limitations, the tissue expression profiles we have observed for *CAX1*::GUS and *CAX3*::GUS are consistent with those determined from both microarray and northern analyses, which also show both contrasting expression patterns for *CAX1* and *CAX3* in addition to overlap in some tissues (Hirschi 1999; Shigaki and Hirschi 2000; Cheng and Hirschi 2003; http://www.cbs.umn.edu/arabidopsis).

A recent study of P-type ATPase heavy metal transporters has several parallels to our findings. Two closely related transporters, *HMA2* and *HMA4*, are differentially expressed in vascular tissues and floral organs. A single-knockout mutation of each transporter does not display any growth defects; however, deletion of both *HMA2* and *HMA4* causes nutritional deficiencies and lethality (Hussain et al., 2004).

CAX1 and CAX3 May Functionally Interact in Yeast

Deregulated versions of CAX1, particularly the truncated versions, have been shown to function in yeast as vacuolar H^+/Ca^{2+} transporters (Hirschi et al., 1996; Pittman and Hirschi, 2001). Here, we show that both full-length CAX1 and CAX3 appear to function as H^+/Ca^{2+} transporters in yeast due to their ability to weakly suppress the Ca^{2+} sensitivity of yeast strains deficient in vacuolar Ca^{2+} transporters (Fig. 3A). We have previously demonstrated that the full-length H^+/Ca^{2+} antiporter from mung bean, VCAX1, can weakly suppress the Ca^{2+} hypersensitivity of K667 yeast, while a truncated version lacking some of the N terminus has much stronger Ca^{2+} transport activity (Pittman et al., 2002b), suggesting that, like VCAX1, full-length CAX1 does have a residual activity and indicating for these two H^+/Ca^{2+} antiporters that the N-terminal region does not completely abolish Ca^{2+} transport but regulates the capacity of Ca^{2+} transport activity. Of note, the deregulated version of CAX3 (sCAX3) does not appear to suppress the Ca^{2+} sensitive phenotypes, hinting at different regulatory modules in this transporter (Shigaki and Hirschi, 2000). When coexpressed, CAX1 and CAX3 can strongly suppress the Ca^{2+} sensitive phenotype (Fig. 3B), suggesting an association between these proteins to alter transport function. This result is intriguing considering that there is specific overlap in the expression profiles of these transporters in planta (Fig. 2). This suggests that CAX1-CAX3 functions as a heteromer only in certain cell types, specifically in parts of the flower, the embryo, and vascular tissue in the root under regular growth condition. *CAX1*::GUS expression is low in the root vasculature, so the occurrence of CAX1-CAX3 association may be less frequent here than in floral tissues. Further work is required to determine whether there are differential cation/H^+ antiport characteristics between CAX1 alone versus the putative CAX1-CAX3 heteromer. It is therefore possible that antiport activity in leaves, where *CAX1* is highly expressed but *CAX3* is undetectable, varies from activity in the flower, where CAX1-CAX3 association may occur. However, from the data in this study, we cannot conclude whether the yeast phenotype conferred by CAX1 and CAX3 coexpression is due to a direct protein-protein interaction. Several studies in both plants and animals have documented heteromeric interactions between related transporters with different kinetic characteristics, which confer novel biological properties that are not seen for each of the transporters individually (Ottschytsch et al., 2002; Reinders et al., 2002; Obrdlik et al., 2004). Future work with the CAX transporters will be needed to determine if the biological effects of coexpression of these transporters are due to direct physical interactions or due to associations that do not involve heterodimerization.

Analysis of *cax3* Lines

To date, we have been unable to directly measure the transport properties of CAX3 by heterologously expressing the transporter in yeast mutants sensitive to Ca^{2+} and other metals (Shigaki and Hirschi, 2000; data not shown). Although full-length CAX3 weakly suppressed the Ca^{2+} sensitivity of the K667 yeast mutant (Fig. 3A), the direct $^{45}Ca^{2+}$ transport assay is not sensitive enough to measure the apparently very low H^+/Ca^{2+} antiport activity of CAX3. The *cax3* lines display no significant alterations in H^+/Ca^{2+} transport when the plants are grown in the presence of exogenous Ca^{2+}, an environmental condition that caused a 50% reduction in H^+/Ca^{2+} in the *cax1* lines (Fig. 5A; Cheng et al., 2003). This experiment indicates that under excess Ca^{2+} stress conditions, unlike CAX1, CAX3 is not a critical Ca^{2+} transporter. Although we may conclude from this that CAX3 does not trans-

port Ca^{2+}, if CAX3 H^+/Ca^{2+} antiport activity is very weak, as found with the yeast transport assay, any change in Ca^{2+} transport activity following *CAX3* deletion may be too small to detect. Alternatively, the lack of reduction in net H^+/Ca^{2+} antiport activity in *cax3* may also be due to up-regulation of additional CAX transporters. However, the *cax3* plants do display a modest, yet significant sensitivity to increased concentrations of Ca^{2+} in the growth media (Fig. 4C), further suggesting that CAX3 in planta does function as a Ca^{2+} transporter, albeit with weak activity. As V-ATPase activity is affected by *CAX1* and *CAX3* deletion, it is possible that the difference in Ca^{2+}/H^+ antiport activity between *cax1* and *cax3* is due in part to a differential ΔpH generated by the V-ATPase. However, for both *cax1* and *cax3*, a similar inhibition of V-ATPase activity was observed, which we assume would disrupt ΔpH across the tonoplast equally in both lines, yet Ca^{2+} transport was significantly reduced only in *cax1*. Further experiments are needed to examine whether alterations in the magnitude of the ΔpH affects cation/H^+ antiport activities by different CAX transporters.

The morphological phenotype of the *cax3* lines are subtle (Fig. 4C). Unlike the *cax1* lines, there is no alteration in root length and flowering time. While the *cax1* lines are slightly more tolerant to an array of metals, including Mn^{2+} and Mg^{2+}, the *cax3* lines, similar to *cax1* (Catala et al., 2003), have a modest sensitivity to Ca^{2+}. Given the reduced V-ATPase activity in the *cax3* lines (Fig. 5B), it is intriguing that we were unable to identify a more pronounced phenotype. Conceivably, a specific stress that we have not yet identified requires CAX3 function.

Analysis of *cax1*/*cax3* Lines

A null mutant of VCX1, the H^+/Ca^{2+} antiporter in yeast, displays normal growth despite these strains lacking all vacuolar Ca^{2+}/H^+ antiport activity (Miseta et al., 1999). In contrast, the Arabidopsis lines that lack both *CAX1* and *CAX3* display dramatic phenotypes while apparently maintaining some H^+/Ca^{2+} transport. However, the environmentally dependent nature of the H^+/Ca^{2+} transport measurements (Fig. 5; see above) suggests that under particular environmental conditions the reduction in transport may be more significant than the 50% measured in these assays. In addition, we suggest that the loss of both CAX1 and CAX3 will abolish the formation of the putative CAX1-CAX3 heteromer (Fig. 3), which may have unique transport functions that are not produced by the single proteins, thereby producing the double-mutant phenotypes.

The 50% reduction in V-ATPase activity in the double mutant is comparable to the 60% reduction in V-ATPase activity reported for the V-ATPase mutant *det3* (Fig. 7B). The *det3* lines display a variety of phenotypes that include reductions in hypocotyl, petiole, and inflorescence stem cell elongation (Schumacher et al., 1999). The question raised here is whether these alterations seen in the *cax1*/*cax3* plants are caused by diminished V-ATPase, by lack of expression of both transporters, or by the loss of transport properties due to the association of CAX1 and CAX3. Future work will test if other *CAX* double mutants are also affected by the changes in the proton gradients, and the severity of the phenotypes in these plants will help.

The *cax1*/*cax3* phenotypes are consistent with the disruption of biochemical functions arising from inadequate supplies of particular elements (see below). For example, the tip burning and stress sensitivities are consistent with Ca^{2+} deficiencies (Marschner, 1995). Previously, we have demonstrated that ectopic expression of deregulated *CAX1* caused increased total Ca^{2+}, but like the *cax1*/*cax3* double mutant, these plants appear Ca^{2+} deficient (Hirschi, 1999). In *S. cerevisiae*, ectopic expression of vacuolar Ca^{2+} transporters causes depletion of the ER Ca^{2+} levels triggering increased influx of Ca^{2+} through PM-localized Ca^{2+} channels (Locke et al., 2000). We speculate that this capacitance calcium entry response is occurring in plants that express high levels of *CAX1*. In other words, increased sequestration into the vacuole is balanced by increasing influx. Conversely, in plants deficient in multiple CAX transporters there may be increased ER pools of Ca^{2+} compared to wild-type plants causing reduced influx of Ca^{2+} through PM channels. Future work will address the cellular distribution of Ca^{2+} using the appropriate in vivo Ca^{2+} indicators (Allen et al., 1999).

CAX and the H^+ Gradient

Previously, we have demonstrated that altered expression of *CAX1* caused altered activity of the V-ATPase (Cheng et al., 2003). Similarly, deletion of *CAX2* reduces V-ATPase activity (Pittman et al., 2004). Here, we demonstrate that modulation of the V-ATPase is not *CAX1* or *CAX2* specific, as alterations in *CAX3* also perturb this proton pump. We have yet to determine the exact mechanisms that allow altered H^+/cation antiport activity to regulate activity of the V-ATPase. Future work will attempt to determine whether direct interactions between the antiporter and ATPase contribute to this regulation. The observation that altered expression of multiple *CAX* transporters (*CAX1*, *CAX2*, and *CAX3*) disrupts V-ATPase activity may suggest an indirect feedback mechanism that is due to the altered H^+ flux across the tonoplast. One possibility is that the deletion of any CAX affects the biosynthesis, assembly, and intracellular trafficking of the subunits of the V-ATPase.

This work does provide insights into how manipulating the expression of a particular antiporter impacts the ensemble of plant transporters. Recently, several labs have reported remarkable phenotypes associated with ectopic expression of vacuolar antiporters (Hirschi, 1999; Shaul et al., 1999; Hirschi et al., 2000; Zhang and Blumwald, 2001). However, if we do not

understand the ramifications of these alterations on the H^+ pumps and H^+ electrochemical gradients (and eventually also manipulate these gradients), the growth and development of these engineered plants will remain unpredictable.

CAX and the Ionome

The dramatic phenotypes and alterations in the ionome of *cax1/cax3* double mutants demonstrate an elaborate interplay between CAX function and the plant's mineral nutrient and trace element composition. These alterations in nutrients may be caused by a direct change in CAX vacuolar cation transport or through indirect changes such as alterations in V-ATPase activity. Alternatively, these changes may be caused by altered expression and activity of other transporters. Alteration in cytosolic Ca^{2+} levels, which we predict to occur following disruption of the vacuolar H^+/Ca^{2+} antiporters, will likely have indirect downstream effects on a variety of proteins including nutrient transporters. Previously, we have shown that *cax1* mutants cause increased expression and activity of other transporters (Cheng et al., 2003). Our recent studies demonstrate only modest alterations in the expression of other transporters (data not shown). Interestingly, the expression of both the low- and high-affinity phosphate transporters and a Ca^{2+}-ATPase ECA1 capable of Ca^{2+} and Mn^{2+} transport are not dramatically increased in the double mutant (data not shown).

The tissues used to analyze transport function and the ionome were different, and care must be taken in our conclusions. The transport data were obtained from root enriched samples where *CAX3* is well expressed. However, the ionome data were from the rosette leaves and *CAX3* is not well expressed in leaf tissue (Fig. 2). Another intriguing aspect of the ionome data is the fluctuation in nutrient levels between the *cax1* and *cax1/cax3* mutants. For example, the *cax1* lines displayed low levels of Mn^{2+} and Zn^{2+}, while the double mutants displayed increased Mn^{2+} and no change in Zn^{2+} levels. We speculate that these fluctuations may result from alterations in the H^+ pumps or due to the lack of association between CAX transporters (Figs. 5 and 7). The ionome data displayed no significant changes in the roots of *cax1/cax3* mutant plants (data not shown). It is important to note that roots were not desorbed with EGTA to remove apoplastic Ca^{2+} but were just rinsed in water. So it is possible that changes in symplastic Ca^{2+} in the double mutant may have been masked by high apoplastic Ca^{2+}.

The necrosis displayed by the *cax1/cax3* double mutant may be caused by the depletion of Ca^{2+} or Mg^{2+} in the plants. Under ideal conditions most plants grow normally with low levels of particular nutrients; but these low levels become inadequate in excessive acidity, or when other anions and cations are present in excess (Fig. 8). The fact that the double mutants can be suppressed by addition of Mg^{2+} and not Ca^{2+} suggests that these defects may be caused by the specific lack of Mg^{2+}. A substantial proportion of the total Mg^{2+} is involved in the regulation of cellular pH and cation-anion balance (Marschner, 1995). In the double mutants, there may be a lack of Mg^{2+} in the vacuole resulting in insufficient Mg^{2+} for charge compensation during particular stress conditions. Certainly an intriguing and unanswered question from our studies is why are Mg^{2+} concentrations low when H^+/Ca^{2+} transporters are deleted? Currently, we have no transport data to suggest the CAX transporters, including CAX1 and CAX3, are capable of Mg^{2+} transport (Shigaki and Hirschi, 2000). Our working hypothesis is that the alterations in nutrients are caused by a general disruption of the association between CAX transporters and the alterations in H^+ pumps.

CONCLUSION

Arabidopsis appears to have several putative CAX transporters (Mäser et al., 2001). Using yeast expression studies, our previous work suggested minimal functional overlap between CAX1 and the closely related transporter CAX3 (Shigaki and Hirschi, 2000). Here, using similar yeast studies, we propose that different CAX transporters may associate, possibly to form heteromers, which confer different biological properties. Although *CAX1* and *CAX3* mutants have subtle morphological phenotypes, we demonstrate that perturbing both *CAX1* and *CAX3* causes significant alterations in plant growth including stunting and tip necrosis. In total, these perturbations cause dramatic alterations in the ionome. Thus, our present genetic studies in planta suggest functional association between the CAX transporters. The future challenge is to delineate the nature of this association and how the action of endomembrane H^+/Ca^{2+} antiporters is integrated into shaping how plants acquire nutrients, grow, develop, and adapt.

MATERIALS AND METHODS

Plasmid DNA Constructs and Plant Transformation

To make transcriptional fusions to GUS reporter genes, *CAX1* and *CAX3* promoter regions upstream of the ATG start codon were amplified from Arabidopsis (*Arabidopsis thaliana*) genomic DNA by PCR using the following primers: forward primer 5′-GAA TTC AAG CTT ACT GCA GTG CAG TTT ACA CAC-3′ and reverse primer 5′-GAA TTC GGA TCC TTC TCT ACT GAC TCA AAA CTT TG-3′ for the *CAX1* promoter; and forward primer 5′-GAA TTC CTC GAG TTT ACA ACT ACA TAA GTT TTG-3′ and reverse primer 5′-GAA TTC GGA TCC GTT TTA AGA CGT TTT GAT TCT AC-3′ for the *CAX3* promoter. The restriction enzyme sites *Hin*dIII, *Xho*I, and *Bam*HI were introduced and underlined. The 2-kb PCR products of *CAX1* and *CAX3* promoter sequences were cloned into the pGEM-T vector (Promega, Madison, WI). The gene promoter fragments were subcloned into the *Hin*dIII/*Bam*HI or *Xho*I/*Bam*HI sites of the pBI121 vector (BD Bioscience CLONTECH, Palo Alto, CA), to replace the cauliflower mosaic virus *35S* promoter and generate the chimeric *CAX1*::*GUS* or *CAX3*::*GUS* constructs.

The triple HA epitope-tagged *CAX3* (*HA-CAX3*) was constructed as previously described (Shigaki et al., 2001). The *HA-CAX3* gene was subcloned into the plant expression vector pBI121, which is driven by a cauliflower mosaic virus 35S promoter.

All the recombinant plasmids and empty vector controls were transformed into *Agrobacterium tumefaciens* GV3101 (Sambrook et al., 1989). These strains were used to transform the Arabidopsis Col-0 using the floral dip method (Clough and Bent, 1998) or tobacco (*Nicotiana tabacum* cv K160) according to published methods (Hirschi, 1999). For Arabidopsis transformation, T_1 seeds were screened on the selection medium and resistance seedlings were transferred to soil, and T_2 seeds were harvested. Homozygous lines were selected by examining the Kan resistance of T_2 seedlings.

Histochemical Assay of GUS Gene Expression

Histochemical assays for *GUS* activity in T3 generation of Arabidopsis transgenic plants harboring *CAX1*::*GUS* or *CAX3*::*GUS*, respectively, were performed according to the protocol described previously (Cheng et al., 2003).

Yeast Strains and Growth

The *Saccharomyces cerevisiae* strain K667 (*cnb1*::*LEU2 pmc1*::*TRP1 vcx1*Δ; Cunningham and Fink, 1996) was used to express vector control and various CAX constructs. Yeast transformation and growth analysis was carried out as previously described (Shigaki et al., 2001).

Membrane Fractionation of HA-CAX3-Expressing Tobacco and Western-Blot Analysis

Microsomal membranes were prepared from HA-CAX3-expressing tobacco leaf tissues as previously described (Cheng et al., 2003). Immunoblots were performed as previously described (Pittman and Hirschi, 2001). The HA epitope and the membrane marker proteins were detected as described previously (Cheng et al., 2003).

Isolation of *CAX3* Knockout Mutants and Creation of *cax1*/*cax3* Double Mutants

To isolate *cax3* null alleles, two T-DNA insertional lines were collected from the SAIL T-DNA insertion collection (Sessions et al., 2002) and the SALK T-DNA insertion collection (Alonso et al., 2003). Homozygous plants from each T3 generation were obtained by PCR screening using *CAX3*-specific and T-DNA border primers. A *CAX3* forward primer, 5′-CTT CCG GGA AGC TGC GTA CAT AGA TGG ACC CAA C-3′, and a T-DNA left border primer, 5′-TAG CAT CTG AAT TTC ATA ACC AAT CTC GAT ACA-3′, were used to screen for the *cax3-1* allele (SAIL line). The *CAX3* forward primer (as above) and a T-DNA right border primer, 5′-TGG GAA AAC CTG GCG TTA CCC AAC TTA AT-3′, were used to screen for the *cax3-2* allele (SALK line). A *CAX3* forward primer (as above) and a *CAX3* reverse primer, 5′-ATT CGC ATG AAA ACA TGA CGT AAC TCT TAG GTA-3′, were used to amplify the wild-type *CAX3* gene. The location of the T-DNA insertion was determined by sequencing of the PCR product. Both *cax3* alleles were backcrossed to their parental plants to remove any potential unlinked mutations. To create *cax1*/*cax3* double-deletion mutants, *cax1-1* and *cax1-2* alleles were crossed with the *cax3-1* allele, and the F_2 generation was selected for *cax1/cax3* double mutant. Homozygous alleles, *cax1-1/cax3-1* and *cax1-2/cax3-1*, were identified by PCR combined with Kan or BASTA resistance selection.

RNA Gel-Blot Analysis

For RNA gel-blot analysis, 3-week-old Arabidopsis wild-type (Col-0) and *cax3* mutant plants were harvested and treated with water (as a control) or 50 mM $CaCl_2$ for 16 h. Total RNA was extracted, blotted, and hybridized with ^{32}P-labeled *CAX3* gene-specific probes as previously described (Cheng et al., 2003).

Plant Materials and Growth Conditions

Arabidopsis Col-0 was used in this study. Wild-type and *cax* single- and double-mutant seeds were surface sterilized, germinated, and grown on one-half-strength MS medium (Murashige and Skoog, 1962) containing 0.5% Suc solidified with 0.8% agar. All plates were sealed with paper surgical tape (Tenderskin, The Kendall Company, Mansfield, MA) and incubated at 22°C under continuous cool-fluorescent illumination for various intervals of time under various environmental conditions. For the ion sensitivity assays, 5-d-old wild-type and *cax* seedlings grown under normal conditions were transferred onto one-half-strength MS media and the identical media supplemented with various metal ions (Cheng et al., 2003). To examine morphological phenotypes of mature wild-type and *cax* single- and double-mutant plants, seeds were sown in artificial soil (Metromix 200, Scotts, Marysville, OH), then kept at 4°C for 2 d to synchronize germination and then grown at 24°C under continuous light. Plants were observed after germination until 6 weeks of age. All photos were taken using a Nikon digital camera (Nikon Coolpix 995, Nikon, Tokyo).

Preparation of Membrane Vesicles and Transport Measurements

Membrane vesicles preparation, Ca^{2+} uptake, and V-ATPase assay were performed as described previously (Cheng et al., 2003).

Preparation of Protoplasts and Visualization of Dye-Loaded Vacuoles

The morphology of the vacuoles (central vacuoles and small vacuoles) in both protoplasts and intact root tissue cells of wild-type and *cax* single- and double-mutant plants was examined as previously described (Cheng et al., 2003).

Ionomic Analysis of *cax* Mutants

Ion profiling was performed as previously described (Lahner et al., 2003). Plants were grown in a climate-controlled room at 19°C to 24°C with 8 h of light at 90 to 150 μE, and plants were misted with 18 MΩ water daily and harvested after 44 d. Plants were grown in Sunshine Mix Number 2 (Sun Gro Horticulture, Baltimore). Plants were bottom watered and fed with 0.25× Hoagland solution at regular intervals. Plants were nondestructively subsampled by removing two to three leaves (0.03–0.14 g fresh weight) and washing with 0.1% Triton X-100 followed by 18 MΩ water before being placed in Pyrex digestion tubes. Digestion was carried out in Pyrex tubes using 1.50 mL concentrated HNO_3 (Fisher TraceMetal grade) at 118°C for 4 h. Each sample was diluted to 16.0 mL with 18 MΩ water and analyzed on a Thermo Elemental PQ ExCell ICP-MS using a glass Conical nebulizer drawing 1 mL per minute. Samples were run twice through the ICP-MS using both hot and cold plasma to measure 18 elements of interest. Beryllium, gallium, and niobium internal standards (EM Science, Gibbstown, NJ), National Institute of Standards and Technology traceable calibration standards (ULTRAScientific, North Kingstown RI), and external drift correction were used. Analysis was performed by ICP-MS for Li^+, B^+, Na^+, Mg^{2+}, PO_4^{3-}, K^+, Ca^{2+}, Mn^{2+}, Fe^{3+}, Co^{2+}, Ni^{2+}, Cu^{2+}, Zn^{2+}, As^{2+}, Se^{2+}, Mo^{2+}, Cd^{2+}, and Pb^{2+}. To increase throughput, sample weights were derived from ICP-MS data by comparing the concentrations of various elements in the sample to those of weighed wild-type controls as described previously (Lahner et al., 2003). In order to perform ICP-MS analysis for root and shoot tissues, the wild-type and mutant seeds were germinated and grown on half-strength MS media under same lighting and growth condition. The root and shoot tissues were harvested after 17-d growth on the medium plates.

ACKNOWLEDGMENTS

We acknowledge the gifts of the polyclonal antibodies against PMA1 and V-PPase from Dr. Ramón Serrano (Heidelberg, Germany) and Dr. Masayoshi Maeshima (Nagoya, Japan), and the monoclonal antibody against V-ATPase from Dr. Heven Sze (College Park, MD). We are grateful to Adam Gillum (Houston) for assistance with the graphics, and are also grateful to the technical assistance of Amanda Brock (Houston).

Received February 12, 2005; revised March 29, 2005; accepted April 25, 2005; published July 29, 2005.

LITERATURE CITED

Allen GJ, Kwak JM, Chu SP, Llopis J, Tsien RY, Harper JF, Schroeder JI (1999) Cameleon calcium indicator reports cytoplasmic calcium dynamics in *Arabidopsis* guard cells. Plant J **19:** 735–747

Alonso JM, Stepanova AN, Leisse TJ, Kim CJ, Chen H, Shinn P, Stevenson DK, Zimmerman J, Barajas P, Cheuk R, et al (2003) Genome-wide insertional mutagenesis of *Arabidopsis thaliana*. Science **301:** 653–657

Carter C, Pan S, Zouhar J, Avila EL, Girke T, Raikhel NV (2004) The vegetative vacuole proteome of *Arabidopsis thaliana* reveals predicted and unexpected proteins. Plant Cell **16:** 3285–3303

Catala R, Santos E, Alonso JM, Ecker JR, Martinez-Zapater JM, Salinas J (2003) Mutations in the Ca^{2+}/H^{+} transporter CAX1 increase CBF/DREB1 expression and the cold-acclimation response in Arabidopsis. Plant Cell **15:** 2940–2951

Cheng NH, Hirschi KD (2003) Cloning and characterization of CXIP1, a novel PICOT domain-containing *Arabidopsis* protein that associates with CAX1. J Biol Chem **278:** 6503–6509

Cheng NH, Pittman JK, Barkla BJ, Shigaki T, Hirschi KD (2003) The Arabidopsis *cax1* mutant exhibits impaired ion homeostasis, development, and hormonal responses, and reveals interplay among vacuolar transporters. Plant Cell **15:** 347–364

Cheng NH, Pittman JK, Shigaki T, Hirschi KD (2002) Characterization of CAX4, an Arabidopsis H^{+}/Ca^{2+} antiporter. Plant Physiol **128:** 1245–1254

Clough SJ, Bent AF (1998) Floral dip: a simplified method for *Agrobacterium*-mediated transformation of *Arabidopsis thaliana*. Plant J **16:** 735–743

Cunningham KW, Fink GR (1996) Calcineurin inhibits *VCX1*-dependent H^{+}/Ca^{2+} exchange and induces Ca^{2+}-ATPases in *Saccharomyces cerevisiae*. Mol Cell Biol **16:** 2226–2237

Epstein E (1972) Mineral Nutrition in Plants: Principles and Perspectives. John Wiley & Sons, New York

Gaxiola RA, Fink GR, Hirschi KD (2002) Genetic manipulation of vacuolar proton pumps and transporters. Plant Physiol **129:** 967–973

Hirschi KD (1999) Expression of Arabidopsis *CAX1* in tobacco: altered calcium homeostasis and increased stress sensitivity. Plant Cell **11:** 2113–2122

Hirschi KD (2003) Insertional mutants: a foundation for assessing gene function. Trends Plant Sci **8:** 205–207

Hirschi KD, Korenkov V, Wilganowski N, Wagner G (2000) Expression of Arabidopsis CAX2 in tobacco: altered metal accumulation and increased manganese tolerance. Plant Physiol **124:** 125–134

Hirschi KD, Zhen R, Cunningham KW, Rea PA, Fink GR (1996) CAX1, an H^{+}/Ca^{2+} antiporter from *Arabidopsis*. Proc Natl Acad Sci USA **93:** 8782–8786

Hussain D, Haydon MJ, Wang Y, Wong E, Sherson SM, Young J, Camakaris J, Harper JF, Cobbett CS (2004) P-type ATPase heavy metal transporters with roles in essential zinc homeostasis in Arabidopsis. Plant Cell **16:** 1327–1339

Lahner B, Gong J, Mahmoudian M, Smith EL, Abid KB, Rogers EE, Guerinot ML, Harper JF, Ward JM, McIntyre L, et al (2003) Genomic scale profiling of nutrient and trace elements in *Arabidopsis* thaliana. Nat Biotechnol **21:** 1215–1221

Leonhardt N, Kwak JM, Robert N, Waner D, Leonhardt G, Schroeder JI (2004) Microarray expression analyses of Arabidopsis guard cells and isolation of a recessive abscisic acid hypersensitive protein phosphatase 2C mutant. Plant Cell **16:** 596–615

Locke EG, Bonilla M, Liang L, Takita Y, Cunningham KW (2000) A homolog of voltage-gated Ca^{2+} channels stimulated by depletion of secretory Ca^{2+} in yeast. Mol Cell Biol **20:** 6686–6694

Marschner H (1995) Mineral Nutrition of Higher Plants. Academic Press, New York

Marty F (1999) Plant Vacuoles. Plant Cell **11:** 587–599

Mäser P, Thomine S, Schroeder JI, Ward JM, Hirschi K, Sze H, Talke IN, Amtmann A, Maathuis FJM, Sanders D, et al (2001) Phylogenetic relationships within cation transporter families of Arabidopsis. Plant Physiol **126:** 1646–1667

Miseta A, Kellermayer R, Aiello DP, Fu L, Bedwell DM (1999) The vacuolar Ca^{2+}/H^{+} exchanger Vcx1p/Hum1p tightly controls cytosolic Ca^{2+} levels in *S. cerevisiae*. FEBS Lett **451:** 132–136

Murashige T, Skoog F (1962) A revised medium for rapid growth and bioassays with tobacco tissue culture. Physiol Plant **15:** 473–497

Obrdlik P, El-Bakkoury M, Hamacher T, Cappellaro C, Vilarino C, Fleischer C, Ellerbrok H, Kamuzinzi R, Ledent V, Blaudez D, et al (2004) K^{+} channel interactions detected by a genetic system optimized for systematic studies of membrane protein interactions. Proc Natl Acad Sci USA **101:** 12242–12247

Ottschytsch N, Raes A, Van Hoorick D, Snyders DJ (2002) Obligatory heterotetramerization of three previously uncharacterized Kv channel alpha-subunits identified in the human genome. Proc Natl Acad Sci USA **99:** 7986–7991

Pittman JK, Hirschi KD (2001) Regulation of CAX1, an Arabidopsis Ca^{2+}/H^{+} antiporter: identification of an N-terminal autoinhibitory domain. Plant Physiol **127:** 1020–1029

Pittman JK, Hirschi KD (2003) Don't shoot the (second) messenger: endomembrane transporters and binding proteins modulate cytosolic Ca^{2+} levels. Curr Opin Plant Biol **6:** 257–262

Pittman JK, Shigaki T, Cheng NH, Hirschi KD (2002a) Mechanism of N-terminal autoinhibition in the *Arabidopsis* Ca^{2+}/H^{+} antiporter CAX1. J Biol Chem **277:** 26452–26459

Pittman JK, Shigaki T, Marshall JL, Morris JL, Cheng NH, Hirschi KD (2004) Functional and regulatory analysis of the *Arabidopsis thaliana* CAX2 cation transporter. Plant Mol Biol **56:** 959–971

Pittman JK, Sreevidya CS, Shigaki T, Ueoka-Nakanishi H, Hirschi KD (2002b) Distinct N-terminal regulatory domains of Ca^{2+}/H^{+} antiporters. Plant Physiol **130:** 1054–1062

Reinders A, Schulze W, Kuhn C, Barker L, Schulz A, Ward JM, Frommer WB (2002) Protein-protein interactions between sucrose transporters of different affinities colocalized in the same enucleate sieve element. Plant Cell **14:** 1567–1577

Sambrook J, Fritsch EF, Maniatis T (1989) Molecular Cloning: A Laboratory Manual. Cold Spring Harbor Laboratory Press, Cold Spring Harbor, NY

Sanders D, Pelloux J, Brownlee C, Harper JF (2002) Calcium at the crossroads of signaling. Plant Cell (Suppl) **14:** S401–S417

Schumacher K, Vafeados D, McCarthy M, Sze H, Wilkins T, Chory J (1999) The *Arabidopsis det3* mutant reveals a central role for the vacuolar H(+)-ATPase in plant growth and development. Genes Dev **13:** 3259–3270

Sessions A, Burke E, Presting G, Aux G, McElver J, Patton D, Dietrich B, Ho P, Bacwaden J, Ko C, et al (2002) A high-through-put *Arabidopsis* reverse genetics system. Plant Cell **14:** 2985–2994

Shaul O, Hilgemann DW, de-Almeida-Engler J, Van Montagu MV, Inze D, Galili G (1999) Cloning and characterization of a novel Mg^{2+}/H^{+} exchanger. EMBO J **18:** 3973–3980

Shigaki T, Cheng NH, Pittman JK, Hirschi KD (2001) Structural determinant of Ca^{2+} transport in the *Arabidopsis* H^{+}/Ca^{2+} antiporter CAX1. J Biol Chem **276:** 43152–43159

Shigaki T, Hirschi KD (2000) Characterization of CAX-like genes in plants: implications for functional diversity. Gene **257:** 291–298

Shigaki T, Sreevidya C, Hirschi KD (2002) Analysis of the Ca^{2+} domain in the *Arabidopsis* H^{+}/Ca^{2+} antiporters CAX1 and CAX3. Plant Mol Biol **50:** 475–483

Sze H, Li X, Palmgren MG (1999) Energization of plant cell membranes by H^{+}-pumping ATPases: regulation and biosynthesis. Plant Cell **11:** 677–689

Sze H, Liang F, Hwang I, Curran AC, Harper JF (2000) Diversity and regulation of Ca^{2+} pumps: Insights from expression in yeast. Annu Rev Plant Physiol Plant Mol Biol **51:** 433–462

Taiz L, Struve I, Rausch T, Bernasconi P, Gogarten JP, Kibak H, Taiz SL (1990) The vacuolar ATPase: structure, evolution, and promoter analysis. *In* RT Leonard, PK Hepler, eds, Calcium in Plant Growth and Development: Current Topics in Plant Physiology, Vol 4. American Society of Plant Physiologists, Rockville, MD, pp 55–59

Ueoka-Nakanishi H, Tsuchiya T, Sasaki M, Nakanishi Y, Cunningham KW, Maeshima M (2000) Functional expression of mung bean Ca^{2+}/H^{+} antiporter in yeast and its intracellular localization in the hypocotyl and tobacco cells. Eur J Biochem **267:** 3090–3098

Villalba JM, Palmgren MG, Berberián GE, Ferguson C, Serrano R (1992) Functional expression of plant plasma membrane H^{+}-ATPase in yeast endoplasmic reticulum. J Biol Chem **267:** 12341–12349

Ward JM, Reinders A, Hsu H-T, Sze H (1992) Dissociation and reassembly of the vacuolar H^{+}-ATPase complex from oat roots. Plant Physiol **99:** 161–169

Zhang HX, Blumwald E (2001) Transgenic salt-tolerant tomato plants accumulate salt in foliage but not in fruit. Nat Biotechnol **19:** 765–768